Asian Journal of Control, Vol. 17, No. 2, pp. 615–625, March 2015
Published online 13 May 2014 in Wiley Online Library (wileyonlinelibrary.com) DOI: 10.1002/asjc.906

A LYAPUNOV BASED MULTI-LEVEL CONTROLLER FOR SEMI-ACTIVE SUSPENSION SYSTEM WITH AN MRF DAMPER

Feng Tyan and Shun-Hsu Tu

ABSTRACT

In this work, we study the implementation of magnetorheological fluid (MRF) to the semi-active suspension. Owing to the nonlinear hysteretic phenomenon, the analysis and synthesis of a controller are not trivial. The kinematic energy and spring potential function of the suspension system plus an integral term of the hysteretic component of an MR damper is chosen as the Lyaupnov function to verify the stability and dissipativity of the system. Then, a multi-level controller, which is constructed in virtue of stability analysis, turns out to be effective in vibration suppression. Through numerical examples, the controller is shown to be robust. In addition, the controller algorithm is simple and easy to implement, requiring only the measurements of relative displacement and velocity between sprung and unsprung masses, along with the damping force of the MR damper.

Key Words: MR damper, semi-active controller, Lyapunov function, dissipativity, quarter vehicle suspension system.

I. INTRODUCTION

For years, vibration attenuation of various dynamic systems has received considerable attention from both academia and industry. In the automobile industry, the perceived comfort level and ride stability of a vehicle are two of the important factors in a subjective evaluation of a vehicle, and the "ride" of a motor vehicle is most commonly measured by the acceleration of the body [1–3]. There are many aspects of a vehicle that influence these two properties, the most important of which are the primary suspension components, which isolate the frame of the vehicle from the axle and wheel assemblies. In the design of a conventional primary suspension system, there always is a trade-off between the two quantities: ride comfort and vehicle handling (safety).

If a primary suspension is designed to optimize the handling and stability of the vehicle, the operator often perceives the ride to be rough and uncomfortable. On the other hand, if the suspension is designed for ride comfort alone, the vehicle may not be stable during maneuvers. As such, the performance of primary suspensions is always defined by the compromise between ride and handling.

The concept of semi-active suspension and semi-active vibration control in connection with the power consumed was introduced by Karnopp [4]. A semi-active suspension consists of a spring and a damper but, unlike a passive suspension, the value of the damper coefficient "c" can be controlled and updated. Various semi-active devices have been proposed to dissipate vibration energy in a structural or vehicle suspension system [5]. The magnetorheological (MR) dampers are new devices that use MR fluid to alter the damping coefficient. These fluids demonstrate dramatic changes in their rheological behaviors in response to a magnetic field.

To control the MR dampers, various control strategies have been proposed in the past two decades, but most of them are either complicated (in the sense of complexity of the algorithm, needing more CPU time, memory, *etc*.) or no direct stability analysis is provided, for example, sliding mode control [6,7] (needs an adequate dynamic reference model), H_∞ control (needs an inverse model of MR damper [8], a state feedback type controller [9], *etc*.), clipped-optimal control [10] (on-off type, needs another desired control force, hence has no direct stability analysis). In contrast, the proposed controller, which is designed to dissipate the system (quarter car and MR damper) energy at the maximum rate, has the feature of simplicity, and it is obtained directly from the stability analysis of the closed-loop suspension system. To reduce the computational burden, the maximum input voltage is divided into finite levels, then the one that maximizes the dissipation of system energy is chosen. In the meantime, the stability analysis also explains why we need the measurements of relative displacement and velocity between sprung and unsprung masses, and the damping force of the MR damper.

This paper is organized as follows. First, we construct the quarter vehicle model with an MR damper utilizing a modified Bouc-Wen model in Section II. Then, the stability analysis is conducted in Section III, after that a multi-level dissipative controller is proposed to suppress the vehicle

Manuscript received April 21, 2013; revised September 11, 2013; accepted November 1, 2013.

Feng Tyan (corresponding author, e-mail: tyanfeng@mail.tku.edu.tw) is with the Computational Dynamics and Control Lab, Dept. of Aerospace Engineering, TamKang University, New Taipei City, Taiwan 25137.

Shun-Hsu Tu is with Sky Leading Corporation, Chupei, Hsin Chu County, Taiwan 30204.

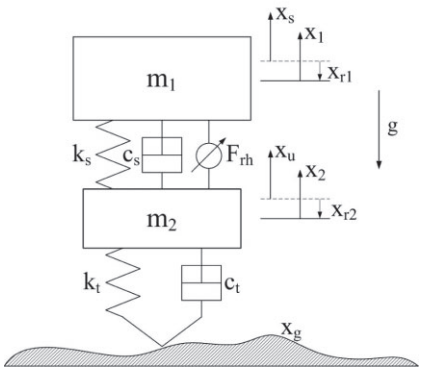

(a) Quarter vehicle suspension model.

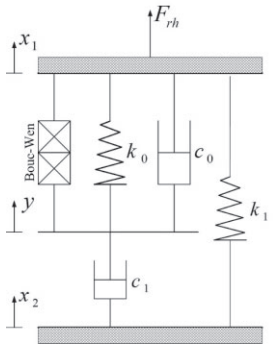

(b) Modified B-W model.

Fig. 1. Quarter vehicle with MR damper suspension system.

vibration. Finally, three numerical examples are used to demonstrate the effectiveness of the controller.

II. QUARTER VEHICLE MODEL WITH MR DAMPER

2.1 Quarter vehicle model

As the vertically oscillating behavior of a vehicle is considered, we investigate the response of vertical dynamics. The response can be described mathematically with a relatively simple set of dynamic equations known as a quarter-car model. The frequency response of the quarter car extends from approximately 0.5 to 20 Hz with some emphasis on roughness at the body bounce frequency and the axle resonance frequency. The rationale favoring the quarter car is the fact that it covers the appropriate frequency range responsible for exciting vehicle vibrations and emphasizes those modal resonances [1].

The equations of motion of the quarter-car model depicted in Fig. 1a can be written as

$$M\ddot{x} + C\dot{x} + Kx = \begin{bmatrix} -1 \\ 1 \end{bmatrix} F_{rh} + \begin{bmatrix} 0 \\ k_t x_g + c_t \dot{x}_g \end{bmatrix}, \tag{1}$$

where the shifted state variables are defined as

$$x = \begin{bmatrix} x_1 \\ x_2 \end{bmatrix} \triangleq \begin{bmatrix} x_s \\ x_u \end{bmatrix} - x_r,$$

in which the reference point, x_r, is the static equilibrium position

$$x_r = \begin{bmatrix} x_{r1} \\ x_{r2} \end{bmatrix} \triangleq K^{-1} \begin{bmatrix} -m_1 \\ -m_2 \end{bmatrix} g = \begin{bmatrix} -\dfrac{m_1 + m_2}{k_t} - \dfrac{m_1}{k_s} \\ -\dfrac{m_1 + m_2}{k_t} \end{bmatrix} g,$$

and the matrices

$$M \triangleq \begin{bmatrix} m_1 & 0 \\ 0 & m_2 \end{bmatrix}, C \triangleq \begin{bmatrix} c_s & -c_s \\ -c_s & c_s + c_t \end{bmatrix},$$
$$K \triangleq \begin{bmatrix} k_s & -k_s \\ -k_s & k_s + k_t \end{bmatrix},$$

in which the quantities

m_1, m_2 are the masses of vehicle body, wheel, and associated components,
x_s, x_u denote vertical displacements of m_1 and m_2,
x_g is the road disturbance,
k_s, c_s represent the stiffness and damping of the uncontrolled suspension, and
k_t, c_t denote the stiffness, damping of the tire.

For convenience, further define the relative state vector:

$$x_P \triangleq \begin{bmatrix} x_{P1} \\ x_{P2} \end{bmatrix} \triangleq \begin{bmatrix} x_1 - x_2 \\ x_2 - x_g \end{bmatrix}.$$

Then the equations of motion can be reformulated as:

$$M_P \ddot{x}_P + C_P \dot{x}_P + K_P x_P = \Lambda F_{rh} - M_P \Gamma \ddot{x}_g, \tag{2}$$

where the transformed matrices are

$$M_P = \begin{bmatrix} m_1 & m_1 \\ m_1 & m_1 + m_2 \end{bmatrix}, C_P = \begin{bmatrix} c_s & 0 \\ 0 & c_t \end{bmatrix}, K_P = \begin{bmatrix} k_s & 0 \\ 0 & k_t \end{bmatrix},$$

and $\Lambda \triangleq [-1 \quad 0]^{\mathrm{T}}, \Gamma \triangleq [0 \quad 1]^{\mathrm{T}}$.

2.2 Modified Bouc-Wen MR damper model

A modified Bouc-Wen model (see Fig. 1b) for predicting the response of the MR damper in the region of the yield point, which was proposed by Spencer [5], is adopted and reformulated as follows:

$$\dot{x}_1 - \dot{y} = \frac{1}{c_0 + c_1} \left[-k_0 (x_1 - y) - \alpha z + c_1 \dot{x}_{P1} \right], \tag{3}$$

$$\dot{z} = (\dot{x}_1 - \dot{y})\left\{\delta - |z|^n[\beta + \gamma\,\mathrm{sgn}(\dot{x}_1 - \dot{y})\,\mathrm{sgn}(z)]\right\}. \quad (4)$$

The force exerted by the MRF damper, F_{rh}, is given by

$$\begin{aligned} F_{rh} &= -c_1(\dot{x}_1 - \dot{y}) + c_1\dot{x}_{P1} + k_1(x_{P1} - \bar{x}_0), \\ &= \frac{c_1}{c_0 + c_1}[k_0(x_1 - y) + \alpha z + c_0\dot{x}_{P1}] + k_1(x_{P1} - \bar{x}_0), \end{aligned} \quad (5)$$

where

$x_1 - y$ and z are the internal relative displacement and hysteretic component of the MR damper, respectively,
$\bar{x}_0$ corresponds to the initial displacement,
δ, β, γ and n are positive constant parameters, and α is a scaling value for Bouc-Wen model, and
k_0, k_1 are spring constants, c_0, c_1 are damping coefficients.

The voltage dependent parameters are modeled by

$$\alpha = \alpha_a + \alpha_b u,\ c_0 = c_{0a} + c_{0b}u,\ c_1 = c_{1a} + c_{1b}u,$$

where α_a, α_b, α_{0a}, α_{0b} and c_{1a}, c_{1b} are positive constants. Furthermore, the command voltage is accounted for through the first-order filter:

$$\dot{u} = -\eta(u - v),\ u(0) = 0, \quad (6)$$

where v is the command voltage sent to the current driver and η is a positive number that reflects the time lag of the MR damper. To reflect the real situation, the command input v is confined to be finite positive. As a result, u is also limited to be positive finite; that is,

$$0 \le v \le V_{\max} \text{ and } 0 \le u \le V_{\max},$$

where $V_{\max}$ is the maximum voltage to the current driver associated with the saturation of the magnetic field in the MR fluid damper. It follows that all of the related parameters α, c_0, and c_1 are all finite positive as well.

Remark 1. The original form for $\dot{y}$ proposed by Spencer was motivated by the force balance, as shown in the following (with moving x_2):

$$\dot{y} = \frac{1}{c_0 + c_1}[k_0(x_1 - y) + \alpha z + c_1\dot{x}_2 + c_0\dot{x}_1].$$

Equations (3)–(5) make it clear that the inputs to the modified Bouc-Wen model are x_{P1}, $\dot{x}_{P1}$ and the state variables are $x_1 - y$ and z.

III. STABILITY ANALYSIS AND CONTROLLER SYNTHESIS

3.1 System stability

Although it is well-known that an MR damper is a dissipative device, to the best of authors' knowledge, a direct proof of this property is still unobtainable. Hence, in this section, we prove this fundamental property of the MR damper when implemented in a vehicle suspension system.

On the $(x_1 - y, z)$-plane, there are two sets of trajectories, which are determined by either one of the following two differential equations:

$$d(x_1 - y) = \frac{dz}{\delta - |z|^n(\beta + \gamma)},$$
$$d(x_1 - y) = \frac{dz}{\delta - |z|^n(\beta - \gamma)}.$$

The "+" or "–" sign between β and γ is determined by the sign of the product $(\dot{x}_1 - \dot{y})z$, while the sign of $\dot{x}_1 - \dot{y}$ is directly controlled by the input to the MR damper, $\dot{x}_{P1}$. For $n = 2$, $\beta - \gamma > 0$, the two corresponding sets of trajectories are

$$x_1 - y = \frac{z_m}{\delta}\tanh^{-1}\frac{z}{z_m} + C_1,$$
$$x_1 - y = \frac{z_M}{\delta}\tanh^{-1}\frac{z}{z_M} + C_2,$$

where C_1 and C_2 are constants that depend on initial conditions, and

$$z_m \triangleq \sqrt[n]{\frac{\delta}{\beta + \gamma}},\ z_M \triangleq \sqrt[n]{\frac{\delta}{\beta - \gamma}}.$$

A general bounded input bounded output (BIBO) stability of the Bouc-Wen model proven in [11] is given in the following lemma, which is needed for the proof of the main theorem, for completeness.

Lemma 1. Consider the MR damper system equation (4) , and let $x_1(t) - y(t)$ be a C^1 input signal.

1. If $\beta - \gamma \le 0$, then $|z(t)| \le \max\{|z(0)|, z_m\}$, $t \ge 0$ for all initial condition $z(0) \in \mathbf{R}$.
2. If $\beta - \gamma > 0$ and the initial condition $|z(0)| \le z_M$, then $|z(t)| \le \max\{|z(0)|, z_m\}$, $t \ge 0$.

The following is the main theorem.

Theorem 1. The quarter-car system (2) with the passive MR damper defined by (3) , (4) , and (5) is dissipative with the supply rate $-[m_1\dot{x}_{P1} + (m_1 + m_2)\dot{x}_{P2}]\ddot{x}_g$, if 1) $\beta - \gamma \le 0$, or 2) $\beta - \gamma > 0$ and $|z(0)| < z_m$.

Proof. Define the Lyapunov candidate function for the quarter car model as

$$V_{qc} \triangleq \frac{1}{2}\dot{x}_P^{\mathrm{T}}M_P\dot{x}_P + \frac{1}{2}x_P^{\mathrm{T}}K_Px_P. \quad (7)$$

It follows immediately that the time derivative of V_{qc} along the system trajectories is

$$\dot{V}_{qc} = -\dot{x}_P^{\mathrm{T}} C_P \dot{x}_P - \dot{x}_{P1} F_{rh} - [m_1 \dot{x}_{P1} + (m_1 + m_2)\dot{x}_{P2}]\ddot{x}_g,$$

where the power consumed by the MR damper can be written in detail as

$$\dot{x}_{P1} F_{rh} = \frac{c_0 c_1}{c_0 + c_1} \dot{x}_{P1}^2 + k_1 \dot{x}_{P1}(x_{P1} - \bar{x}_0) + \frac{c_1 \dot{x}_{P1}}{c_0 + c_1}[k_0(x_1 - y) + \alpha z].$$

Two cases are considered in the following.

Case 1. $\beta - \gamma \le 0$: A naive choice of the Lyapunov candidate function for the MR damper is

$$V_{rh} \triangleq \frac{1}{2} k_1 (x_{P1} - \bar{x}_0)^2 + \frac{1}{2} k_0 (x_1 - y)^2 + \int_0^z \frac{\alpha}{\delta} z dz. \tag{8}$$

It can be shown that

$$\dot{V}_{rh} = \dot{x}_{P1} F_{rh} + \dot{V}_a - \frac{\alpha}{\delta} z(\dot{x}_1 - \dot{y})|z|^n [\beta + \gamma \operatorname{sgn}(\dot{x}_1 - \dot{y}) \operatorname{sgn}(z)],$$

where $\dot{V}_a \triangleq -c_{rh} \dot{x}_{P1}^2 - \frac{1}{c_0 + c_1}[k_0(x_1 - y) + \alpha z]^2$, and $c_{rh} \triangleq \frac{c_0 c_1}{c_0 + c_1}$. Then, let the Lyapunov candidate function for the quarter car and suspension system be:

$$V = V_{qc} + V_{rh}.$$

It follows that

$$\dot{V} + [m_1 \dot{x}_{P1} + (m_1 + m_2)\dot{x}_{P2}]\ddot{x}_g = -\dot{x}_P^T C_P \dot{x}_P + \dot{V}_a - \frac{\alpha}{\delta} z(\dot{x}_1 - \dot{y})|z|^n [\beta + \gamma \operatorname{sgn}(z(\dot{x}_1 - \dot{y}))] \le 0.$$

This is because the third term in the above is negative when $z(\dot{x}_1 - \dot{y})$ is either positive or negative.

Case 2. $\beta - \gamma > 0, |z(0)| < z_m$: In this case, a Lyapunov candidate function for the MR damper is chosen to be:

$$V_{rh} \triangleq \frac{1}{2} k_1 (x_{P1} - \bar{x}_0)^2 + \frac{1}{2} k_0 (x_1 - y)^2 + \int_0^z \frac{\alpha z}{\delta} \left\{ 1 + \frac{|z|^n [\beta + \gamma \operatorname{sgn}(z(\dot{x}_1 - \dot{y}))]}{\delta - |z|^n [\beta + \gamma \operatorname{sgn}(z(\dot{x}_1 - \dot{y}))]} \right\} dz. \tag{9}$$

Since $|z(0)| < z_m$, according to Lemma 1, we have $|z(t)| \le z_m$ for all $t \ge 0$, which assures the (local) positive definiteness of V_{rh}. It can be shown that

$$\dot{V}_{rh} = \dot{x}_{P1} F_{rh} + \dot{V}_a,$$

which renders

$$\dot{V} + [m_1 \dot{x}_{P1} + (m_1 + m_2)\dot{x}_{P2}]\ddot{x}_g = -\dot{x}_P^T C_P \dot{x}_P + \dot{V}_a \le 0. \tag{10}$$

From the above two cases, we conclude that system (2) is dissipative with respect to supplied rate $-[m_1 \dot{x}_{P1} + (m_1 + m_2)\dot{x}_{P2}]\ddot{x}_g$ under the given conditions. ▪

Remark 2. It is worthy to point out that, in Case 1 of Theorem 1, if the initial condition of z satisfies $|z(0)| < z_m$, then the Lyapunov function (9) can also be adopted in this case, which in turn yields the same time derivative $\dot{V}$ as given by (10).

3.2 A Lyapunov function based multi-level damper controller

From a practical perspective, it is reasonable to assume that $|z(0)| < z_m$; hence, the Lyapunov function (9) is adopted for controller synthesis. The implementation of (5) to the second term on the right hand side of (10) renders:

$$\dot{V}_a = \dot{V}_a(x_{P1}, \dot{x}_{P1}, F_{rh}, u) = -\frac{c_0}{c_1 c_{rh}}[F_{rh} - c_{rh}\dot{x}_{P1} - k_1(x_{P1} - \bar{x}_0)]^2 - c_{rh}\dot{x}_{P1}^2.$$

The above expression suggests that the input function v take the form

$$v = v(x_{P1}, \dot{x}_{P1}, F_{rh}, u),$$

which indicates that the measurements needed for constructing the feedback controller are the relative displacement, x_{P1}, and velocity, $\dot{x}_{P1}$, between the sprung and unsprung masses of vehicle, and the damping force, F_{rh}, of MR damper. While the input voltage u is determined by minimizing the augmented function $\dot{V}_a$, that is to dissipate the system energy ($V_{qc} + V_{rh}$) as fast as possible. Owing to the fast dynamics of the command voltage (6) , it is fair to assume that $u = v$. Hence, a simple multi-level controller is proposed as follows:

$$v = \frac{i}{N} V_{\max} \text{ such that } \dot{V}_a\left(x_{P1}, \dot{x}_{P1}, F_{rh}, \frac{i}{N} V_{\max}\right) \text{ is minimized, for } i \in \{0, 1, \ldots, N\}, \tag{11}$$

where N is the number of levels that the input voltage is divided into. To have a smooth input voltage, a first order filter, $\frac{1}{\tau_v s + 1}$, may be augmented to the damper controller. Simulink block diagrams for the closed-loop system and controller are given in Fig. 2 to illustrate the usage of the proposed controller.

Remark 3. Implementing the first equation of (1) and the second equation of (2) on (10) yield:

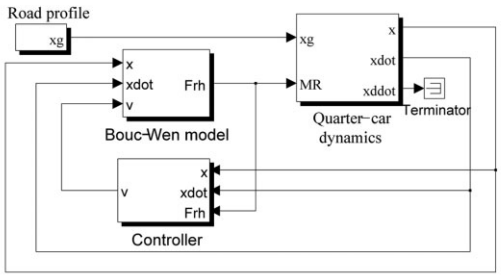

(a) Closed-loop system configuration.

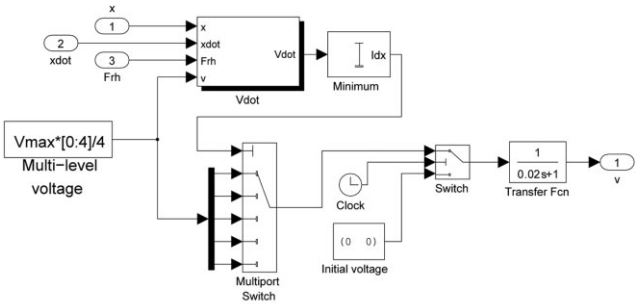

(b) Controller (11) for $N = 4$.

Fig. 2. Simulink block diagrams for closed-loop system configuration.

Table I. Quarter-car model parameters [7].

Parameter	Value
m_1	372 kg
m_2	45 kg
k_s	40 kN/m
k_t	190 kN/m
c_s	0 N s/m
c_t	0 N s/m

Table II. Parameters for the MR damper RD-1005-1 [7].

Coeff.		Coeff.	
α_a	12441 N/m	c_{0_a}	784 N s/m
α_b	38430 N/m V	c_{0_b}	1803 N s/m V
β	2059020 m^{-2}	c_{1_a}	14649 N s/m
γ	136320 m^{-2}	c_{1_b}	34622 N s/m V
δ	58	n	2
η	190 s^{-1}	$\bar{x}_0$	0 m
k_0	3610 N/m	k_1	840 N/m

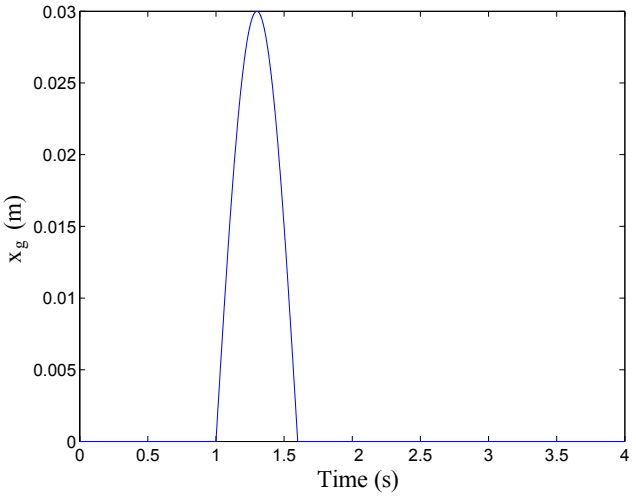

(a) Bump excitation.

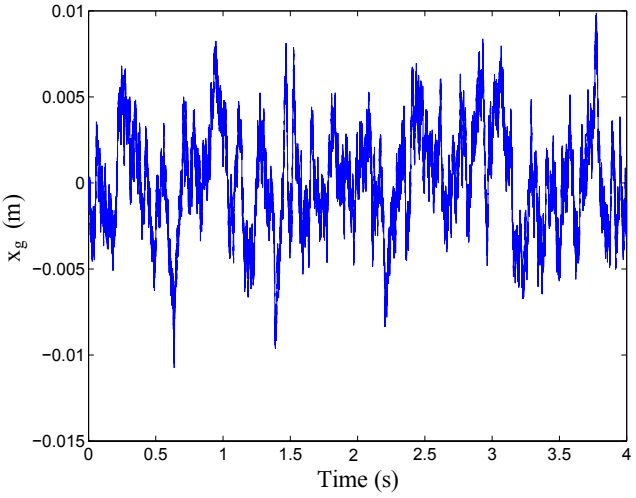

(b) Grade C random road profile.

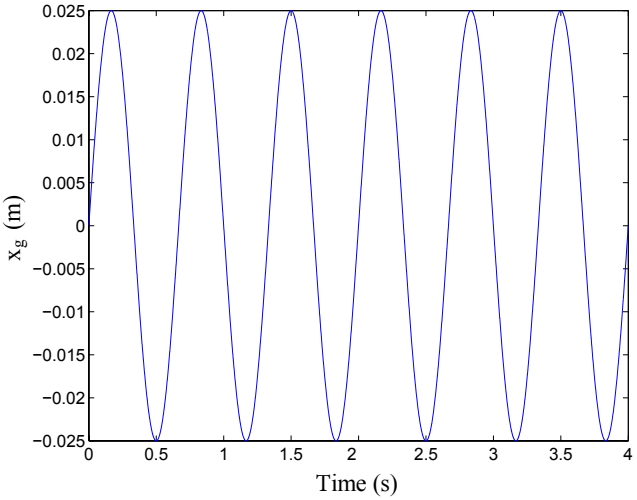

(c) Sinusoidal road profile.

Fig. 3. Road profiles.

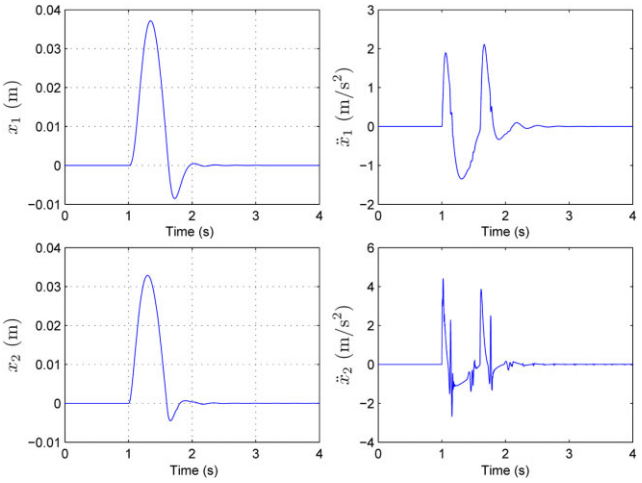

Fig. 4. Responses of sprung and unsprung masses of the quarter car model with an MR damper and multi-level controller under bump excitation when c_0 is replaced by $0.85c_0$, c_1 by $0.75c_1$, and k_1 by $0.80k_1$ in $\dot{V}_a$.

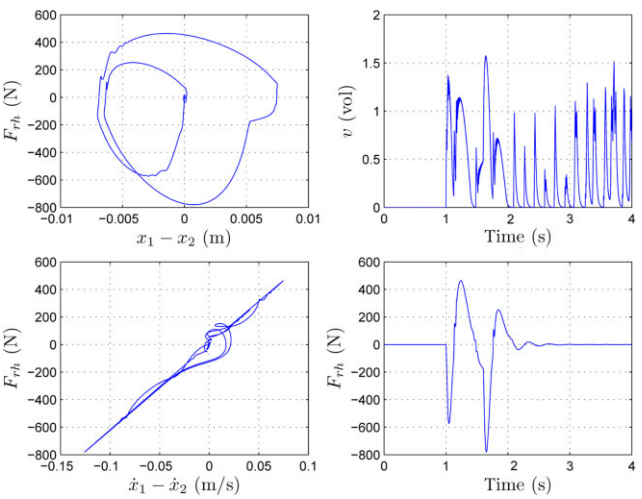

Fig. 5. Damping force and input voltage of MR damper with multi-level controller when c_0 is replaced by $0.85c_0$, c_1 by $0.75c_1$, and k_1 by $0.80k_1$ in $\dot{V}_a$.

$$
\begin{aligned}
&\dot{V} + [m_1\dot{x}_{P1} + (m_1+m_2)\dot{x}_{P2}]\ddot{x}_g \\
&\quad = -\frac{c_s + c_{rh}}{c_s^2}\left[m_1\ddot{x}_1 + k_s x_{P1} + F_{rh}\right]^2 \\
&\qquad - \frac{1}{c_t}\left[m_1\ddot{x}_1 + k_t x_{P2} + m_2\ddot{x}_2\right]^2 \\
&\qquad - \frac{c_0 + c_1}{c_1^2}\left[\frac{c_{rh}m_1}{c_s}\ddot{x}_1 + \left(\frac{c_{rh}k_s}{c_s} - k_1\right)x_{p1}\right. \\
&\qquad \left. + \left(1 + \frac{c_{rh}}{c_s}\right)F_{rh} + k_1\bar{x}_0\right]^2 \\
&\quad = -\zeta^{\mathrm{T}} Q \zeta,
\end{aligned}
\tag{12}
$$

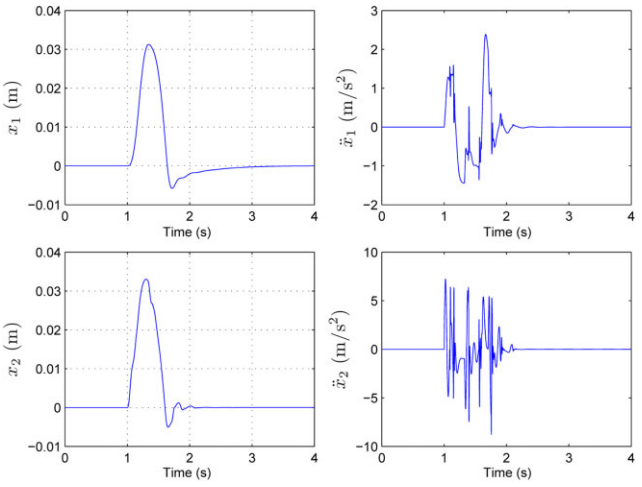

Fig. 6. Responses of sprung and unsprung masses of the quarter-car model under bump excitation for skyhook controller with $c_{sky} = 100$.

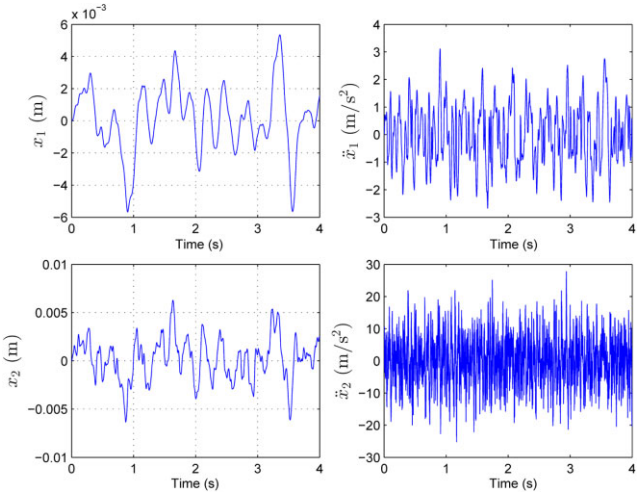

Fig. 7. System response of the quarter-car vehicle model with an MR damper and a Lyapunov based multi-level controller when subject to a Grade C random road excitation.

where $\zeta \triangleq [\ddot{x}_1 \quad x_{P1} \quad x_{P2} \quad \ddot{x}_2 \quad F_{rh} \quad \bar{x}_0]^{\mathrm{T}}$, and Q is the corresponding positive semi-definite matrix. This indicates that the minimized quadratic performance index is indeed the linear combination of $\ddot{x}_1$ (corresponding to ride comfort), x_{P1} (corresponding to suspension deflection), x_{P2} (corresponding to road holding ability), $\ddot{x}_2$ (wheel acceleration), and the MR damper force F_{rh}.

Then, integrating (12) from $t = 0$ to $t = T$ results in:

$$
V(T) - V(0) + \int_0^T [m_1\dot{x}_{P1} + (m_1+m_2)\dot{x}_{P2}]\ddot{x}_g dt = -\int_0^T \zeta^{\mathrm{T}} Q \zeta dt.
$$

Dividing the above equation by $\int_0^T [m_1\dot{x}_{P1} + (m_1+m_2)\dot{x}_{P2}]\ddot{x}_g dt$ and choosing $V(0) = 0$ give:

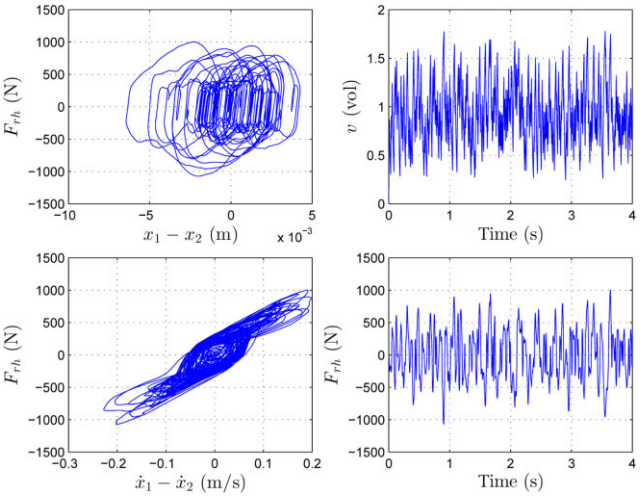

Fig. 8. Damping force and input voltage of an MR damper with a Lyapunov based multi-level controller when subject to sinusoidal road excitation.

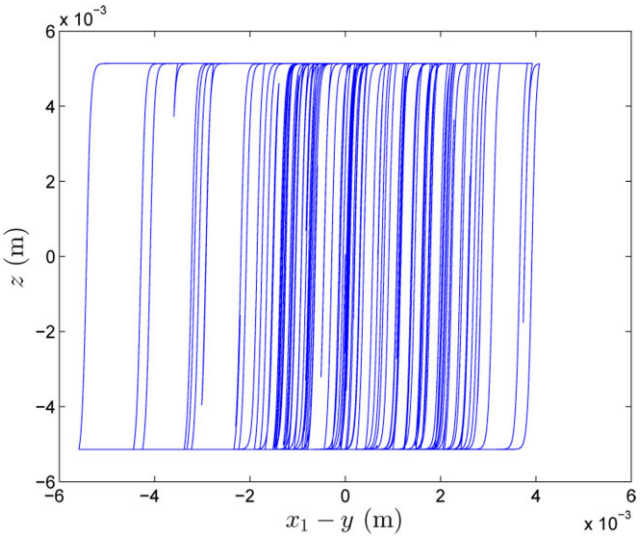

Fig. 9. Phase plot of ($x_1 - y$, z) of an MR damper with a Lyapunov based multi-level controller when subject to a Grade C random road excitation.

Table III. RMS analysis for Grade C road excitation tests ((11)*: in $\dot{V}_a$ replace c_0 by $0.85c_0$, c_1 by $0.75c_1$, k_1 by $0.80k_1$.)

Controller	$\ddot{x}_1$ (m/s^2)	x_{P1}(m)	x_{P2}(m)
$v = 0$	0.6706	0.0035	0.0030
$v = 2$	1.4009	0.0017	0.0030
Skyhook ($c_{sky} = 100$)	0.8840	0.0027	0.0028
(11)*	1.0952	0.0019	0.0025

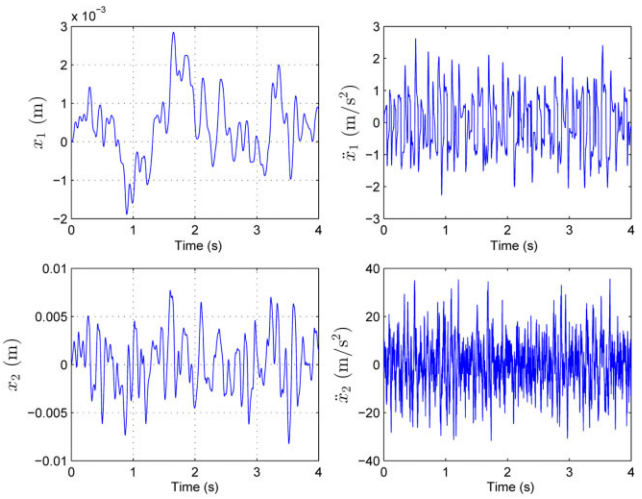

Fig. 10. System response of the quarter-car vehicle model with MR damper and a skyhook controller when subject to a Grade C random road excitation.

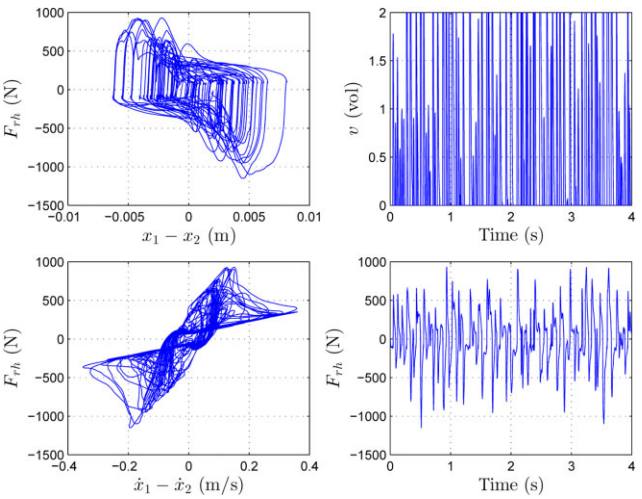

Fig. 11. Damping force and input voltage of an MR damper with a skyhook controller when subject to a Grade C random road excitation.

$$\frac{\int_0^T \zeta^{\mathrm{T}} Q \zeta dt}{-\int_0^T [m_1 \dot{x}_{P1} + (m_1 + m_2)\dot{x}_{P2}]\ddot{x}_g dt} = 1 + \frac{V(T)}{\int_0^T [m_1 \dot{x}_{P1} + (m_1 + m_2)\dot{x}_{P2}]\ddot{x}_g dt}. \tag{13}$$

Note that $V(T) \geq 0, \forall T > 0$. If the input energy $-\int_0^T [m_1 \dot{x}_{P1} + (m_1 + m_2)\dot{x}_{P2}]\ddot{x}_g dt > 0$, then the ratio between output and input energy is given by

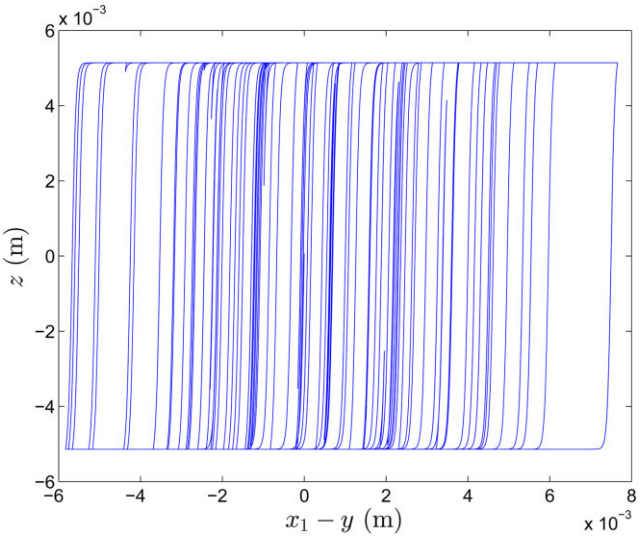

Fig. 12. Phase plot of $(x_1 - y, z)$ of an MR damper with a skyhook controller when subject to a Grade C random road excitation.

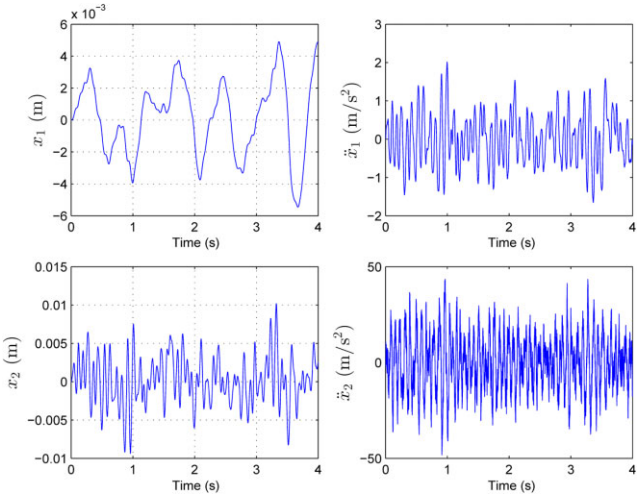

Fig. 13. System response of the quarter-car vehicle model with MR damper and a constant input voltage $v = 0$ when subject to a Grade C random road excitation.

$$0 \le \frac{\int_0^T \zeta^{\mathrm{T}} Q \zeta dt}{-\int_0^T [m_1 \dot{x}_{P1} + (m_1 + m_2)\dot{x}_{P2}]\ddot{x}_g dt} \le 1, \tag{14}$$

while if $-\int_0^T [m_1 \dot{x}_{P1} + (m_1 + m_2)\dot{x}_{P2}]\ddot{x}_g dt < 0$, we have

$$0 \ge \frac{\int_0^T \zeta^{\mathrm{T}} Q \zeta dt}{-\int_0^T [m_1 \dot{x}_{P1} + (m_1 + m_2)\dot{x}_{P2}]\ddot{x}_g dt} \ge 1,$$

which is impossible. Consequently, the above analysis indicates that the constructed controller is also robust in the sense that the H_∞ norm [9] like function (14) is smaller than or equal to 1.

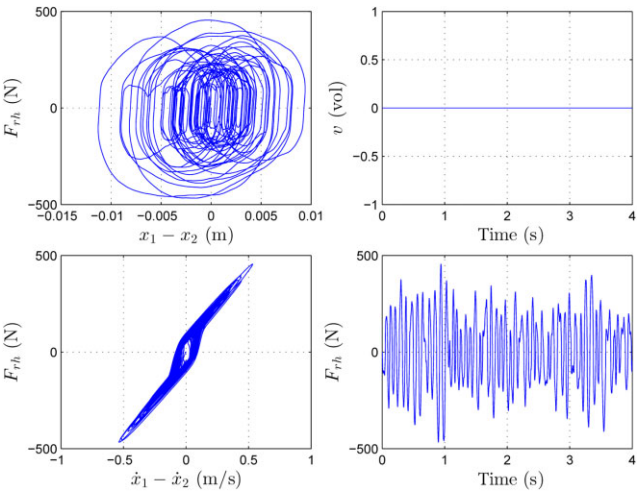

Fig. 14. Damping force and input voltage of an MR damper with a constant input voltage $v = 0$ when subject to a Grade C random road excitation.

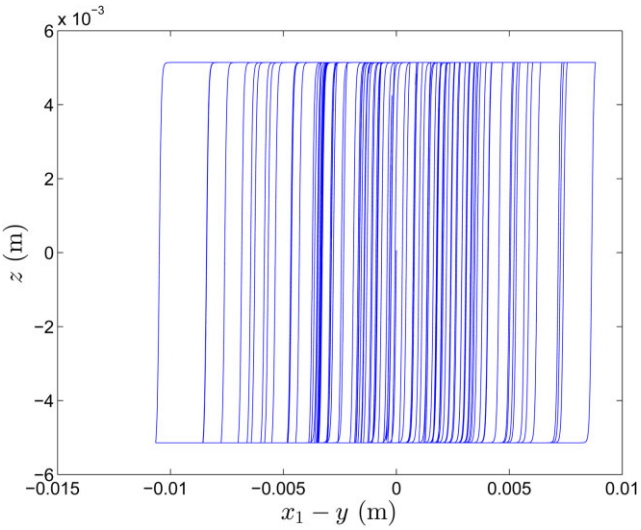

Fig. 15. Phase plot of $(x_1 - y, z)$ of an MR damper with a constant voltage $v - 0$ when subject to a Grade C random road excitation.

IV. NUMERICAL EXAMPLE

Consider the quarter car and an MR damper model with the parameters defined by Tables I and II, respectively [7]. Assume that the maximum input voltage of the MR damper is $V_{\max} = 2.0$V. Three kinds of road profile inputs are considered in this example (see Fig. 3).

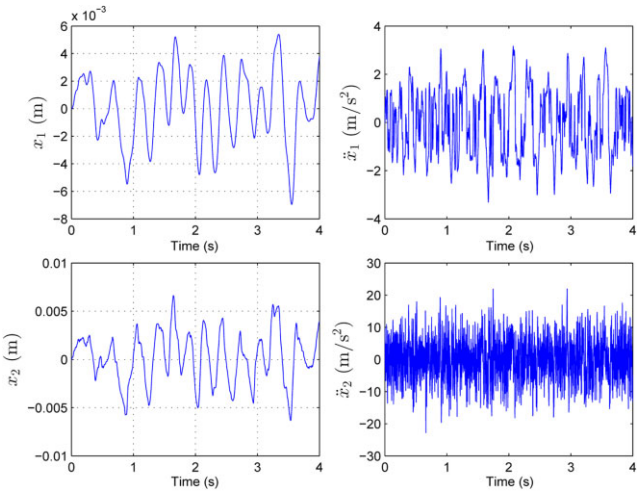

Fig. 16. System response of the quarter-car vehicle model with MR damper and a constant input voltage $v = 2$ when subject to a Grade C random road excitation.

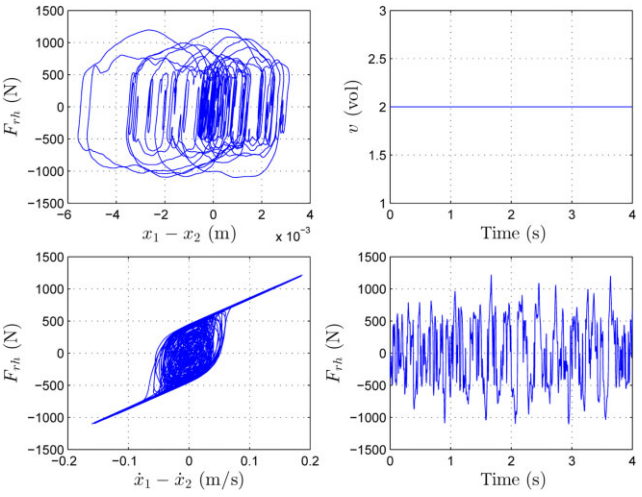

Fig. 17. Damping force and input voltage of an MR damper with a constant input voltage $v = 2$ when subject to a Grade C random road excitation.

4.1 Case I: 0.03 m height bump disturbance

Let the vehicle be subject to a bump excitation with amplitude 0.03 m, as shown in Fig. 3a. Then, we implement the above controller (11) along with a first-order filter in the system, and let $N = 4$, $\tau_v = 0.02$ seconds. To demonstrate the robustness of the proposed controller, for illustration purposes, in $\dot{V}_a$ of (11) , we replace c_0 by $0.85c_0$, c_1 by $0.75c_1$, and k_1 by $0.80k_1$. The corresponding responses of sprung mass and unsprung mass, force, and input voltage history are shown in Figs 4 and 5 . Note that the "ride" of a motor vehicle is most commonly measured by the acceleration on the body [1,2]. For comparison purposes, the responses of the case with a skyhook controller

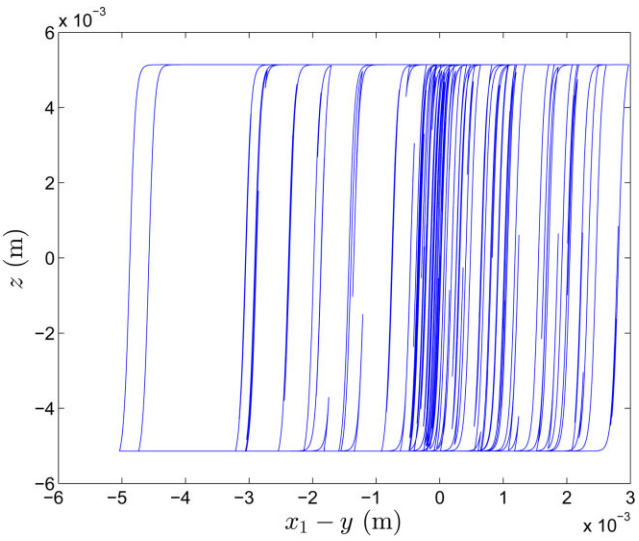

Fig. 18. Phase plot of $(x_1 - y, z)$ of an MR damper with a constant voltage $v = 2$ when subject to a Grade C random road excitation.

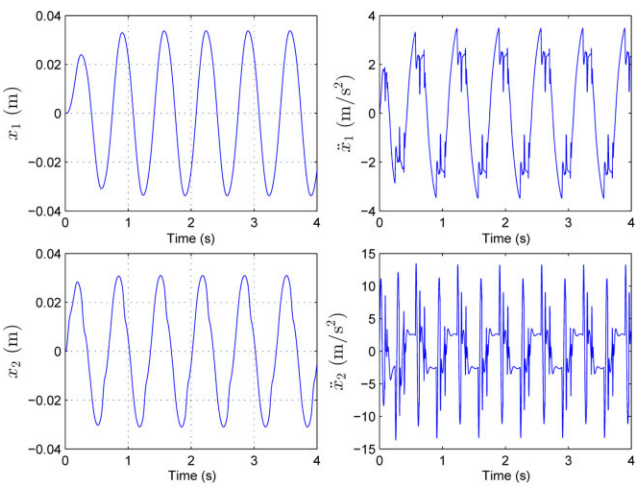

Fig. 19. System response of the quarter-car vehicle model with an MR damper and a skyhook controller when subject to a sinusoidal road excitation.

$$v = \begin{cases} c_{sky}|\dot{x}_1|, & \dot{x}_1\dot{x}_{P1} \geq 0, \\ 0, & \text{otherwise.} \end{cases} \tag{15}$$

are given in Fig. 6 (in which $c_{sky} = 100$ for better matching the responses of sprung mass in Fig. 4). As we can tell from the given results, the proposed controller leads to a smaller acceleration of unsprung mass. In addition, compared to the results shown in [7], the controller (11) outperforms that of [7], in the sense of having less settling time and having smaller peak values of response and acceleration of sprung mass. In addition, the proposed algorithm is simple, and no reference model is required.

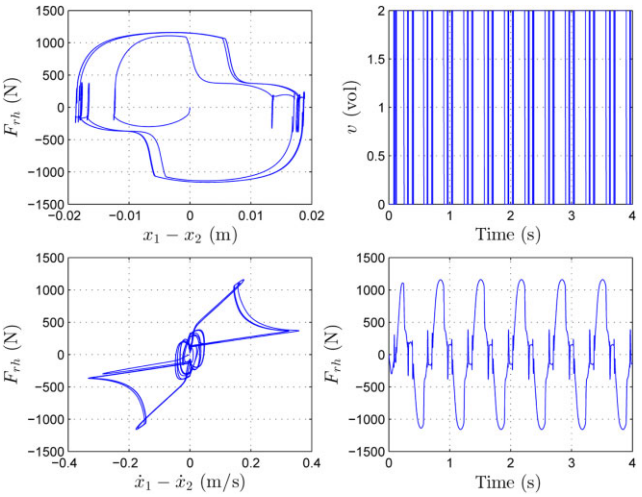

Fig. 20. Damping force and input voltage of an MR damper with a skyhook controller when subject to a sinusoidal road excitation.

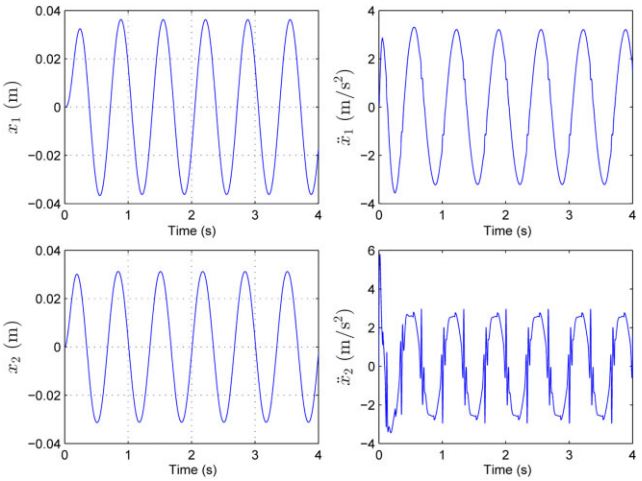

Fig. 21. System Response of the quarter car vehicle model with an MR damper and a Lyapunov based multi-level controller when subject to a sinusoidal road excitation.

4.2 Case II: Grade C random road profile

In this case, a Grade C road profile [12], shown in Fig. 3b is given as the random excitation to the suspension system. The resulting system response and force history are given in Figs. 7 and 8, respectively. In addition, the internal state variables ($x_1 - y, z$) are depicted in Fig. 9. The maximum value of z is 0.0051, which agrees with z_m, as defined in the proof of Theorem 1. Some typical values of the RMS of the acceleration of the spring, the suspension deflection ($x_{P1} = x_1 - x_2$), and the tyre deflection ($x_{P2} = x_2 - x_g$) for the listed four different cases are given in Table III. The results for skyhook controller and constant input voltage $v = 0$, $v = 2$ controllers are also given in Figs 10–18 for reference. These

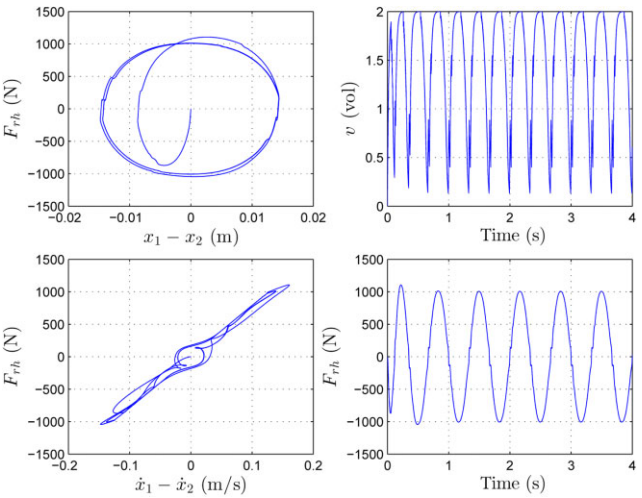

Fig. 22. Damping force and input voltage of an MR damper with a Lyapunov based multi-level controller when subject to a sinusoidal road excitation.

results indicate that the proposed controller provides acceptable performance, which emphasizes the suppression of suspension deflection (x_{P1}) (as we have expected) and road holding ability (tyre deflection, x_{P2}), while the commonly used skyhook controller focuses on the ride comfort ($\ddot{x}_1$).

4.3 Case III: Sinusoidal road profile

For the time domain analysis, a sinusoidal road input at 1.5Hz was chosen to represent the steady-state analysis because this frequency is very close to the natural frequency of the sprung mass. For the 1.5Hz signal, a peak-to-peak amplitude of 5cm was chosen, $x_g = 0.025\sin(3\pi t)$. This amplitude was limited by the stroke of the MR damper. At this amplitude, the travel across the damper was approaching the end-stops of the damper. Figs 19–22 show time response of displacement of sprungmass m_1 and acceleration for a sinusoidal road input for skyhook and the proposed multi-level controller. In addition, the RMS values of the results are also given in Table IV for passive off ($v = 0$), passive on ($v = 2$), skyhook controller, and the proposed controller (11) . This table indicates that the suspension system cannot be stabilized with the passive off type controller and the skyhook controller focuses on the ride comfort again.

V. CONCLUSIONS AND FUTURE WORKS

In this work, a Lyapunov function, consisting of the kinematic energy and spring potential function of a suspension system plus an integral term of the hysteretic component of an MR damper is chosen to examine the stability and dissipativity of a system. To suppress the vibration, a multi-level controller based on the derivative of the Lyapunov

Table IV. RMS analysis for sinusoidal road excitation $x_g = 0.025\sin(3\pi t)$.

Controller	$\ddot{x}_1$ (m/s^2)	x_{P1}(m)	x_{P2}(m)
$v = 0$	7.8620	0.0649	0.0159
$v = 2$	2.33	0.0086	0.0050
skyhook ($c_{sky} = 100$)	2.1620	0.0137	0.0047
(11)	2.3026	0.0100	0.0049

function is proposed. It requires only the measurements of relative displacement and velocity between sprung and unsprung masses, the damping force, and the voltage dependent coefficients c_0, c_1 and k_1, which can be identified in the beginning. Through numerical examples, the proposed controller turns out to be effective, robust, and the algorithm is simple to implement. These results indicate that this controller emphasizes the suppression of suspension deflection and road holding ability, while the skyhook controller focuses on the ride comfort. To have a compromise between all three performance indices, a hybrid control policy can be considered. In the future, the effects on the parameter uncertainties will be further investigated.

REFERENCES

1. Gillespie, T. D., "Everything you always wanted to know about the IRI, but were afraid to ask!" The University of Michigan Transportation Research Institute, Lincoln, Nebraska, Road Profile Users Group Meeting (1992).
2. Sam, Y. M. and J. H. S. B. Osman, "Modeling and control of the active suspension system using proportional integral sliding mode approach," *Asian J. Control*, Vol. 7, No. 2, pp. 91–98 (2005).
3. Gáspár, P., Z. Szabó, G. Szederkényi, and J. Bokor, "Design of a two-level controller for an active suspension system," *Asian J. Control*, Vol. 14, No. 3, pp. 664–678 (2012).
4. Karnopp, D., M. J. Crosby, and R. A. Harwood, "Vibration control using semi-active force generators," *J. Eng. Ind.*, Vol. 96, pp. 619–626 (1974).
5. Spencer, B. Jr., S. Dyke, M. Sain, and J. Carlson, "Phenomenological model for magnetorheological dampers," *J. Eng. Mechanics*, Vol. 123, No. 3, pp. 230–238 (1997).
6. Yokoyama, M., J. K. Hedrick, and S. Toyama, "A model following sliding mode controller for semi-active suspension systems with MR dampers," in *Proceedings of the American Control Conference*, Arlington, VA, pp. 2652–2657 (2001).
7. Lam, A. H.-F. and W.-H. Liao, "Semi-active control of automotive suspension systems with magnetorheological dampers," *Int. J. Veh. Des.*, Vol. 33, No. 1–3, pp. 50–75 (2003).
8. Du, H., K. Y. Sze, and J. Lam, "Semi-active H_∞ control of vehicle suspension with magnetorheological dampers," *J. Sound Vibr.*, Vol. 283, No. 3–5, pp. 981–996 (2005).
9. Tyan, F., S.-H. Tu, and W. S. Jeng, "Semi-active augmented H_∞ control of vehicle suspension systems with MR dampers," *J. Chin. Soc. Mech. Eng.*, Vol. 29, No. 3, pp. 249–255 (2008).
10. Dyke, S. J., B. F. Spencer, M. K. Sain, and J. D. Carison, "Modeling and control of magnetorheological dampers for seismic response reduction," *Smart Mater. Struct.*, Vol. 5, No. 5, pp. 565–575 (1996).
11. Ikhouane, F., V. M. Nosa, and J. Rodellar, "Bounded and dissipative solutions of the bouc-wen model for hysteretic structural systems," in *Proceedings of the American Control Conference*, Vol. 4, No. 4, Boston, MA, USA, pp. 3520–3525 (2004).
12. Tyan, F., Y.-F. Hong, S.-H. Tu, and W. S. Jeng, "Generation of random road profiles," *J. Advanced Eng.*, Vol. 4, No. 2, pp. 151–156 (2009).

Feng Tyan received his Ph.D. degree in aerospace engineering from the University of Michigan, Ann Arbor, in 1995. From 1989 to 1991, he worked as a software engineer at Mechanical Dynamics INC., Ann Arbor, Michigan. Since 1995 he has been with the Tamkang University, where he is presently a faculty in the Department of Aerospace Engineering. His research interests are in the areas of guidance, estimation, robust control, nonlinear control theory, and computational dynamics.